

## Compensation techniques for experimental errors in real-time hybrid simulation using shake tables

Narutoshi Nakata<sup>1\*</sup> and Matthew Stehman<sup>2a</sup>

<sup>1</sup>Department of Civil and Env. Engineering, Clarkson University, 8 Clarkson Ave., Potsdam, NY 13699, USA

<sup>2</sup>Department of Civil Engineering, Johns Hopkins University, 3400 N. Charles, St., Baltimore, MD 21218, USA

(Received April 14, 2014, Revised June 8, 2014, Accepted August 10, 2014)

**Abstract.** Substructure shake table testing is a class of real-time hybrid simulation (RTHS). It combines shake table tests of substructures with real-time computational simulation of the remaining part of the structure to assess dynamic response of the entire structure. Unlike in the conventional hybrid simulation, substructure shake table testing imposes acceleration compatibilities at substructure boundaries. However, acceleration tracking of shake tables is extremely challenging, and it is not possible to produce perfect acceleration tracking without time delay. If responses of the experimental substructure have high correlation with ground accelerations, response errors are inevitably induced by the erroneous input acceleration. Feeding the erroneous responses into the RTHS procedure will deteriorate the simulation results. This study presents a set of techniques to enable reliable substructure shake table testing. The developed techniques include compensation techniques for errors induced by imperfect input acceleration of shake tables, model-based actuator delay compensation with state observer, and force correction to eliminate process and measurement noises. These techniques are experimentally investigated through RTHS using a uni-axial shake table and three-story steel frame structure at the Johns Hopkins University. The simulation results showed that substructure shake table testing with the developed compensation techniques provides an accurate and reliable means to simulate the dynamic responses of the entire structure under earthquake excitations.

**Keywords:** real-time hybrid simulation; substructure shake table testing; acceleration tracking; actuator delay compensation; force correction in hybrid simulation

### 1. Introduction

Real-time hybrid simulation (RTHS) is a promising new experimental technique that enables systems-level performance assessment of structures at the true dynamic loading rate. It was expanded upon from pseudo-dynamic testing incorporating real-time computational process and dynamic hydraulic actuators (Nakashima *et al.* 1992). In RTHS, responses of entire structural systems are simulated combining computational models and physical tests; in general, only structural members of which responses are difficult to model are experimentally tested. Thus, RTHS offers a cost-effective means for performance assessment of entire structural systems with

---

\*Corresponding author, Associate Professor, E-mail: [nnakata@clarkson.edu](mailto:nnakata@clarkson.edu)

<sup>a</sup> Graduate Student, E-mail: [mstehma1@jhu.edu](mailto:mstehma1@jhu.edu)

fully incorporated physical tests of structural members. In particular, RTHS is advantageous for simulations of systems with rate-dependent structural members that are not accurately evaluated by the conventional slow-speed hybrid simulation. Those structural members include dampers (Christenson *et al.* 2008, Carrion *et al.* 2009, Zapateiro *et al.* 2010) and bearings (Pan *et al.* 2005 and Igarashi *et al.* 2009), etc. Although the advantages of RTHS have been recognized by many earthquake engineers, research efforts on RTHS are still limited to date. Further advances in methodologies and more applications are needed to promote this emerging experimental technique.

One of the attractive RTHS techniques is one that utilizes shake tables. If shake tables are available and their controllers allow external control, RTHS systems can be developed as an extension to existing facilities. Because shake table systems include most of the essential components for RTHS, including dynamic actuators, servo controllers, data acquisition, etc., the required cost for the upgrade is not even comparable to the investment for an entire new RTHS system. Most importantly, RTHS using shake tables provides a lot of potential to enhance capabilities and applications of shake table tests such as testing of high-rise buildings and soil-structure interaction studies, etc.

Ideas to use shake tables for RTHS and related research efforts can be found in literature. Igarashi *et al.* (2000) proposed a substructure shake table test method for a study of tuned mass dampers (TMD). In their study, a TMD was experimentally tested on a shake table while a single-degree-of-freedom structure was computationally simulated. A great deal of research on control issues in real-time substructuring experiments has been conducted at the University of Bristol. Stoten and Gomez (2001) and Neild *et al.* (2005) demonstrated that the adaptive minimal control synthesis (MCS) controller improved the displacement tracking in real-time substructure tests using a shake table. Lee *et al.* (2007) proposed a real-time substructuring technique for the shake table test of upper substructures. They adopted the inverse transfer function technique to improve the distortion of the interface acceleration. Some studies investigated substructure shake table testing with a middle or lower part of the structure on shake table. Shao *et al.* (2011) developed a system to test a middle part of the structure on a shake table utilizing an auxiliary actuator to impose the interaction force from the upper part. Nakata and Stehman (2012) proposed a substructure shake table test system with a use of inertial masses to incorporate the interaction force. Stability and feasibility of the substructure shake table tests with inertial masses are numerically investigated. An example of RTHS for a real structural system was reported by Gunay and Mosalam (2012). They developed a real-time hybrid simulation framework for efficient dynamic testing of electrical insulator posts and validated the framework through a comparison with shake table tests of the entire system including the high voltage electrical switch and the insulator posts. Though it is not hybrid simulation, Ji *et al.* (2009) is worth mentioning as an interesting application of the substructure shake table testing. They developed a rubber-and-mass system between a full-scale shake table and a physical model of upper floors in a high-rise building. Their system was utilized to amplify the shake table motion to reproduce large floor responses in the high-rise building.

As briefly introduced here, RTHS using shake tables has attracted great attention from researchers. However, methodologies for RTHS using shake tables have not yet matured. For example, almost all of the experimental substructures tested in RTHS using shake tables are very simple such that the effects of the test structure on control system (a.k.a, control-structure interaction, Dyke *et al.* 1995) are either negligible or can be easily compensated in an outer-loop controller such as inverse compensation technique (Lee *et al.* 2007, Spencer and Yang 1998).

When complex and heavy structures, such as several floors of a high-rise building, are tested on a shake table, the control-structure interaction becomes significant. Even with advanced compensation techniques for actuators (Nakata 2010, Phillips and Spencer 2011, Stehman and Nakata 2012), it is certainly not possible to completely avoid acceleration tracking errors. If test structures have high correlation with the input ground acceleration, such acceleration tracking errors propagate through the dynamics of the structure and inevitably induce erroneous responses. Feeding the erroneous responses into the RTHS procedure will deteriorate the RTHS results. To enhance the capabilities of RTHS using shake tables, techniques to compensate for response errors induced by the imperfect input acceleration are critical and essential.

This study presents a set of techniques to enable accurate and reliable RTHS using shake tables. The developed techniques include compensation techniques for errors induced by imperfect input acceleration of shake tables, model-based actuator delay compensation with state observer, and force correction to eliminate process and measurement noises. These techniques are experimentally verified through RTHS using a uni-axial shake table and three-story steel frame structure at the Johns Hopkins University. Details of the developed techniques and test results are presented in this paper

## 2. Background of real-time hybrid simulation using shake tables

In this study, we consider RTHS where the lower part of the structure is computationally simulated while the upper part of the structure is experimentally tested on a shake table. Just for convenience of naming, we simply refer to RTHS using shake tables as substructure shake table testing in the rest of the paper. To derive compatibility requirements, this section presents the underlying dynamics of substructure shake table testing.

### 2.1 Equations of motion

Fig. 1 shows two schematics of a multistory building subjected to earthquake ground motions: (a) entire system and (b) substructure system. The entire system is an  $n$ -story shear-type building where the dynamic response is viewed as a reference for the substructure system. The equations of motion for each floor of the entire system can be expressed as

$$m_i \ddot{x}_i + R_i(\dot{d}_i, d_i) - R_{i+1}(\dot{d}_{i+1}, d_{i+1}) = -m_i \ddot{x}_g \quad (i = 1, \dots, n \text{ and } R_{n+1} = 0) \tag{1}$$

where  $m_i$  is the mass of the  $i$ -th floor;  $x_i$  is the  $i$ -th floor relative displacement with respect to the ground;  $d_i$  is the  $i$ -th floor story drift that can be expressed as  $x_i - x_{i-1}$ ;  $R_i$  is the  $i$ -th floor nonlinear restoring force including damping; and  $\ddot{x}_g$  is the ground acceleration. Note that  $R_i$  is the function of the relative story velocity,  $\dot{x}_i - \dot{x}_{i-1}$ , and the story drift,  $x_i - x_{i-1}$ . In the entire simulation, the ground acceleration is the only input to the dynamic system.

The entire structure is divided into two structures in the substructure system:  $n_c$ -story computational substructure and  $n_e$ -story experimental substructure that represent the lower and upper parts of the entire system, respectively ( $n = n_c + n_e$ ). The equations of motion of the substructure system can be expressed as

$$m_{c\_i}\ddot{x}_{c\_i} + R_{c\_i}(\dot{d}_{c\_i}, d_{c\_i}) - R_{c\_i+1}(\dot{d}_{c\_i+1}, d_{c\_i+1}) = -m_{c\_i}\ddot{x}_{g\_c} \quad (i=1, \dots, n_c-1) \tag{2}$$

$$m_{c\_i}\ddot{x}_{c\_i} + R_{c\_i}(\dot{d}_{c\_i}, d_{c\_i}) - f_{c\_n_c} = -m_{c\_i}\ddot{x}_{g\_c} \quad (i=n_c) \tag{3}$$

$$m_{e\_i}\ddot{x}_{e\_i} + R_{e\_i}(\dot{d}_{e\_i}, d_{e\_i}) - R_{e\_i+1}(\dot{d}_{e\_i+1}, d_{e\_i+1}) = -m_{e\_i}\ddot{x}_{g\_e} \quad (i=1, \dots, n_e \text{ and } R_{e\_n_e+1}=0) \tag{4}$$

where  $m_{c\_i}$  and  $m_{e\_i}$  are the  $i$ -th floor mass of the computational and experimental substructures, respectively;  $x_{c\_i}$  and  $x_{e\_i}$  are the  $i$ -th floor relative displacement of the computational and experimental substructures, respectively;  $d_{c\_i}$  and  $d_{e\_i}$  are the  $i$ -th floor story drift of the computational and experimental substructures, respectively;  $R_{c\_i}$  and  $R_{e\_i}$  are the  $i$ -th floor nonlinear restoring force of the computational and experimental substructures, respectively; and  $\ddot{x}_{g\_c}$  and  $\ddot{x}_{g\_e}$  are the ground acceleration of the computational and experimental substructures, respectively; and  $f_{c\_n_c}$  is the interaction force from the experimental substructure at the  $n_c$ -th floor of the computational substructure. In the substructure system, Eq. (2) is solved solely computationally while Eq. (3) incorporates the interaction force  $f_{c\_n_c}$  from experiments. Eq. (4) should be experimentally evaluated using a shake table.

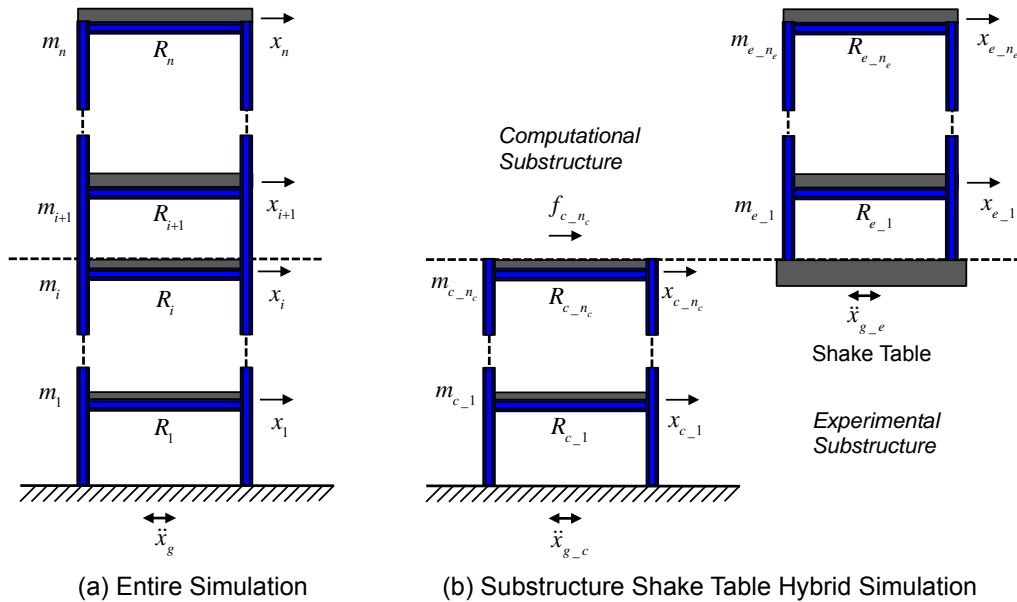


Fig. 1 Schematics of substructure shake table testing in comparison with the entire simulation

### 2.2 Compatibility requirements

For the substructure system to have the equivalent dynamics as the entire system, model assumptions have to be clarified and compatibility conditions have to be identified. To address issues associated with RTHS techniques, model properties in the entire and substructure systems are assumed identical in this study. That is,  $m_{c\_i} = m_i$  and  $R_{c\_i} = R_i$  for  $i = 1, \dots, n_c$ , and  $m_{e\_i} = m_{i+n_c}$  and  $R_{e\_i} = R_{i+n_c}$  for  $i = 1, \dots, n_e$ .

With the above model assumptions, the remaining conditions that have to be satisfied are input compatibility conditions. First, the input ground acceleration to the computational substructure has to be the same as the one to the entire system (computational acceleration compatibility), that is

$$\ddot{x}_{g\_c} = \ddot{x}_g \tag{5}$$

The computational acceleration compatibility is straight forward since the input ground acceleration in the computational substructure is known in advance and can be directly incorporated in the computational simulation.

Second, the input acceleration to the experimental substructure has to be the absolute acceleration at the top floor of the computational substructure (experimental acceleration compatibility), that is

$$\ddot{x}_{g\_e} = \ddot{x}_{c\_n_c} + \ddot{x}_{g\_c} \tag{6}$$

The experimental acceleration compatibility implies that the reference ground acceleration to the shake table is not known in advance and has to be accurately imposed in the experimental process.

Finally, the interaction force at the top floor of the computational substructure has to be equal to the base shear in the experimental substructure (interface force compatibility), that is

$$f_{c\_n_c} = R_{e\_1}(\dot{d}_{e\_1}, d_{e\_1}) \tag{7}$$

The interface force compatibility requires accurate measurement or estimation of the base shear in the experimental substructure during shake table tests. All of these compatibility conditions (Eqs. (5)-(7)) have to be satisfied at any given instance during the simulation.

### 2.3 Concept of substructure shake table testing

A block diagram of the concept for substructure shake table testing is shown in Fig. 2. The entire process of substructure shake table testing can be described by two blocks with input-output relations. The first block represents a computational process that simulates response of the computational substructure from two inputs, the ground acceleration and the interaction force from the experimental substructure. The output from the computational process is the top floor absolute acceleration of the computational substructure that is sent to the experimental process as the input. Then, the experimental process imposes this acceleration to the experimental substructure using a shake table. The base shear in the experimental substructure is treated as the output in the experimental process and should be sent back to the computational process as the interaction force.

As shown here, the concept of substructure shake table testing is rather simple. However, actual implementation with computational and experimental processes is challenging. Required techniques to enable substructure shake table testing, RTHS using shake tables, are those that ensure accurate data processing in the block diagram without errors and time delays.

### 3. Experimental setup and structural models

To develop the required techniques to enable RTHS using shake tables, this study utilizes an experimental setup at the Johns Hopkins University. Fig. 3 shows a photo of the experimental set up. The setup consists of a uniaxial shake table; a three-story steel frame structure as the experimental substructure; and control and data acquisition systems. In addition to the description of the experimental setup, this section presents experimentally identified dynamic properties of the shake table and the experimental substructures as well as parameters for the computational model.

#### 3.1 Uni-axial shake table

The shake table has a 1.2 m x 1.2 m aluminum platform driven by a Shore Western hydraulic actuator (Model: 911D). The actuator has a dynamic load capacity of 27 kN and a maximum stroke limit of  $\pm 7.6$  cm. An MTS 252 series dynamic servo valve is used to control the fluid flow through the actuator chambers. The specifications of the shake table are: maximum velocity of  $\pm 5.1$  cm/s, maximum acceleration of 3.8 g; and maximum payload of 1.0 ton. The actuator is equipped with an embedded displacement transducer and an inline load cell to measure the force on the actuator. A general-purpose accelerometer is installed on the table to measure absolute acceleration of the shake table.

#### 3.2 Control and data acquisition system

The control hardware for the shake table includes a National Instruments 2.3 GHz high-bandwidth dual-core PXI express controller (PXIe-8130), a windows-based host PC and other accessories. The data acquisition system consists of a 16-bit high-speed multifunction data acquisition board (PXI-6251), a signal conditioner (SCXI-1000), and various analog input modules. Programs for the control and data acquisition are written in NI LabVIEW, and are deployed on a real-time operating system on the PXIe-8130. The PXIe-8130 is a real-time controller that is capable of running multiple independent digital processes up to 10 kHz. The integrated control and data acquisition system enables simultaneous sampling of all of the input and output signals, and user-defined control and signal processes. More details of the control and data acquisition system as well as the shake table can be found in Nakata (2011).

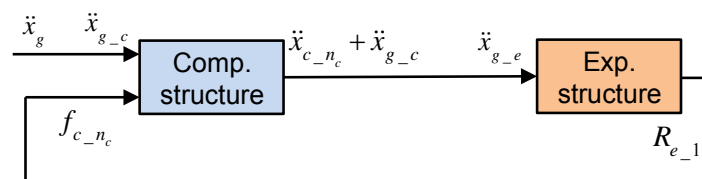


Fig. 2 A block diagram for the concept of substructure shake table testing

### 3.3 Experimental substructure

The experimental substructure is a 700 mm tall three-story steel frame with a floor size of 304 mm x 610 mm. Each floor has four identical steel columns (5.08 cm wide W8x13 I-beams) that are bolted to the floors. At each floor, five steel plates are placed as an additional masses of 90.7 kg. The total mass of the structure including columns and support connections is approximately 300 kg, that is more than double the mass of the shake table platform.

Dynamic properties of the experimental substructure are examined using a band-limited white noise excitation from the shake table. Fig. 4 shows the frequency response curves from the shake table acceleration to the absolute floor accelerations. Distinct peaks appear at 6.9 Hz, 21.9 Hz, and 34.5 Hz in all of the transfer functions, indicating the first, second, and third natural frequencies of the experimental substructure, respectively. Damping ratios for the first, second, and third vibration modes are 1.1%, 0.8%, and 2.8%, respectively. In this study, it is assumed that the structure remains linear elastic during the experiments; however the concept of substructure shake testing is still valid for nonlinear test structures.



Fig. 3 A three-story steel frame structure on the uni-axial shake table at Johns Hopkins University

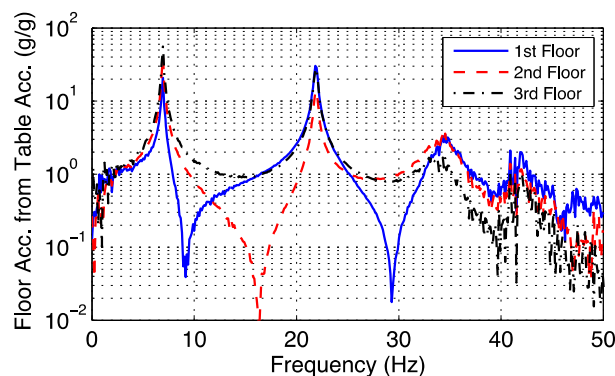


Fig. 4 Frequency response curves of the three-story steel experimental substructure

Table 1 Dynamic properties of the entire structural model for RTHS using shake tables

Mode	Natural Frequencies	Damping Ratios
1 <sup>st</sup>	2.52 Hz	7.76 %
2 <sup>nd</sup>	6.80 Hz	11.11%
3 <sup>rd</sup>	9.60 Hz	19.28 %

### 3.4 Computational substructure

The computational substructure is a linear elastic seven-story shear building with the story mass of 226 kg, floor stiffness of  $1.76 \times 10^3$  kN/m, and floor damping coefficient of 17.6 kN s/m. The first three natural frequencies of the computational structure are 2.92 Hz, 8.64 Hz, and 14.0 Hz, and the corresponding damping ratios are 9.2 %, 27.2%, and 43.9 %, respectively. Combined with the experimental substructure, the entire structural model has the dynamic properties listed in Table 1.

### 3.5 Measurement of base shear

Measurement of the base shear from the experimental substructure is required for the interface force compatibility in substructure shake table testing. However, the base shear is not directly measured in the current test setup; in order to directly measure, load cells need to be installed either between the base of the structure and the shake table or all of the columns. In this study, the base shear is obtained as the sum of the inertial forces of the upper floors (i.e., sum of the mass times absolute floor acceleration) as

$$R_{e-1} = - \sum_{i=1}^3 m_{e-i} (\ddot{x}_{e-i} + \ddot{x}_{g-e}) \quad (8)$$

The above form can be derived from the sum of the equations of motion in Eq. (4). It should be mentioned that this approach is valid only for lumped mass systems of which dynamic responses can be expressed in the equations of motion in Eq. (4). Because the experimental setup herein has significant mass at each floor, the lumped mass assumption is considered appropriate.

It is worth mentioning that another approach for the measurement of the base shear is examined in this study using the force measurement from the load cell on the actuator and the table acceleration. However, the load cell is subjected to inevitable friction between the bearings and the linear guides of the shake table. Therefore, this study adopts the base shear that is obtained using the absolute floor accelerations.

## 4. Acceleration control performance and influence of input acceleration error on structural responses

To meet the experimental acceleration compatibility in substructure shake table testing, shake

tables have to provide perfect tracking of the absolute top floor acceleration of the computational substructure. However, acceleration control of shake tables is extremely difficult mainly due to limitations in displacement control (Twitchell and Symans 2003) and control-structure interaction (Dyke *et al.* 1995). Prior to implementation of substructure shake table testing, a preliminary investigation of acceleration control performance and influence of input acceleration errors on structural responses is performed.

#### 4.1 Issues of acceleration control and control-structure interaction

While shake tables are designed to produce reference accelerations, primary controllers, inner-loop servo controllers, for actuators are displacement control. In almost all the cases, the inner-loop servo controllers are proportional-integral-derivative (PID) controllers or PID with additional feedbacks (e.g., differential pressure feedback). In practice, a command shaping controller/filter such as the inverse dynamics compensation techniques is added to cancel out the dynamics of the inner-loop control system (Spencer and Yang 1998). Basically, command shaping is an off-line process that alters the reference displacements to produce the closest possible reference accelerations. To assess a possible use of such command shaping techniques for substructure shake table testing, the control performance of the shake table with the experimental substructure is discussed.

Fig. 5 shows the frequency response curves (FRC) of the closed-loop (reference to measured) displacement (a and c) and the closed-loop (reference to measured) acceleration (b and d) at the proportional gain of 8.5. For a reference, the FRCs of bare table at the proportional gain of 20 are shown in the plots. As shown in the magnitude plots, the bare table FRCs provide relatively smooth, wide and flat regions in both displacement and acceleration. Because of their smoothness, the magnitude responses in both displacement and acceleration are possibly improved up to around 25 Hz with a low-order inverse compensation technique. On the other hand, the FRCs with the experimental substructure show peculiar responses in both displacement and acceleration with pairs of peaks and valleys around 7 Hz and 22 Hz. These frequencies correspond to the first and the second natural frequencies of the experimental substructure, indicating significant control-structure interaction. As a result, the reliable band-width of the acceleration FRC is limited to 6 Hz. The reason that the gain has to be lower than the gain for the bare table is because of stability; due to the spike and the phase drop at 7 Hz, the phase margin becomes much smaller than that of the bare table. This stability assessment is also confirmed experimentally with uncontrollable 7 Hz vibration that occurs at the proportional gain of higher than 8.5. Therefore, the inner-loop control performance in displacement and acceleration cannot be further improved with a tuning of PID gains.

An application of the inverse compensation techniques is examined. However, it turns out that because of uncertainties in the high frequency range and inability to compensate for the complex dynamic characteristics of the closed-loop responses without introducing further delay, alteration of the reference displacement will amplify vibration at the first and second natural frequencies of the structure. Because of these reasons, the proportional controller with the gain of 8.5 is the only controller used in this study. The characteristics of the acceleration FRC in Fig. 5 indicate that input acceleration errors are present in this control system.

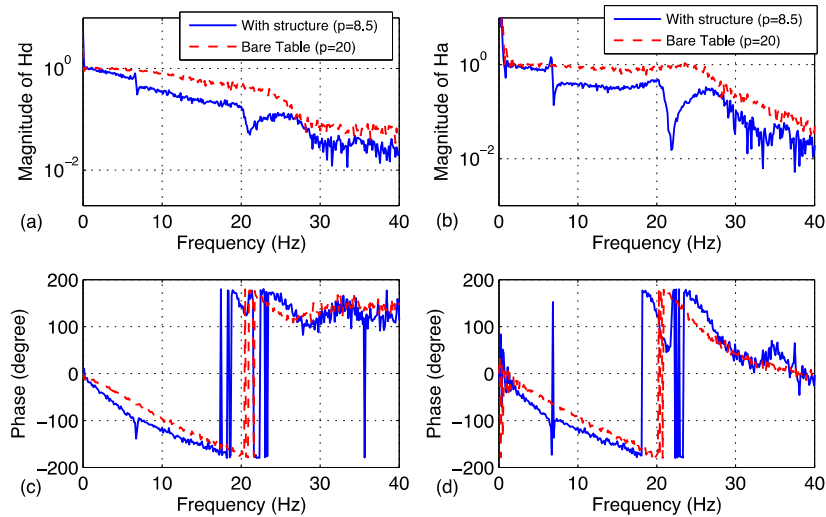


Fig. 5 Frequency response curves of closed-loop (reference to measured) displacement and acceleration: (a) displacement magnitude; (b) acceleration magnitude; (c) displacement phase; and (d) acceleration phase

#### 4.2 Propagation of input acceleration errors

To assess the possible response errors induced by the erroneous input acceleration, the dynamic relationship between the input acceleration and the base shear are discussed. Fig. 6 shows the frequency response curves and coherence of the base shear from the table acceleration. The magnitude plot in Fig. 6(a) shows distinct peaks at the natural frequencies of the experimental substructure. The phase plot in Fig. 6(b) exhibits that the phase characteristics of the base shear has a complex relation with that of the table acceleration. These dynamic characteristics of the base shear are similar to those of the floor accelerations in Fig. 4, indicating the relationship between the input acceleration and the base shear is a multi-degrees-of-freedom dynamic system. Most importantly, the acceleration-base shear relationship is highly correlated up to 40 Hz as shown in Fig. 6(c). This highly correlated dynamic relationship reveals that input acceleration error will propagate and appear in the base shear measurement with amplified magnitude and varying phase characteristics depending on its frequency contents.

### 5. Substructure shake table test system with error compensation

All of the compatibility requirements have to be satisfied during real-time computational and experimental processes in the substructure shake table test. However, as discussed in the previous section, errors in the input acceleration and the base shear are inevitable in the experimental process. To enable accurate dynamic response analysis of the entire structure through the substructure shake table test, those errors have to be properly compensated for. This section presents a complete set of techniques developed for substructure shake table testing that

compensate for errors in the experimental acceleration and interface force compatibilities.

Fig. 7 shows a schematic of the substructure shake table test system with the compensation techniques for experimental errors. The overall system consists of a computational simulation of the computational substructure; measurement force corrector; state estimator for the experimental substructure; and actuator delay compensation for the shake table. Details of each process are discussed herein.

### 5.1 Numerical integration for the computational substructure

A numerical solution algorithm is an essential component in RTHS to solve governing equations of motion. In the conventional hybrid simulation, only restoring forces are experimentally evaluated while the rest of the entire structure including the mass and damping of the experimental substructure are simulated computationally. Therefore, equations of motion for the entire structure, Eqs. (2)-(4), can be solved with an estimated stiffness of the experimental structure. The Newmark family and predictor-corrector type numerical integration algorithms (e.g., alpha-OS) are often used to solve for the future response of the entire structure and specify the reference displacement. In the case of the substructure shake table testing, all of the dynamic effects of the experimental substructure including inertia, damping and stiffness terms are experimentally incorporated. Therefore, it makes more logical sense to solve for the response of only computational substructure in the numerical algorithm incorporating the interface force from the experimental substructure as an additional input. Solutions for such dynamic processes can be obtained using a discrete-time state space approach.

The procedure for the computational substructure is as follows. Given that the state vector  $\mathbf{x}_c$  and the input vector  $\mathbf{u}_c$  are available at the  $j$ -th step, the output vector  $\mathbf{y}_c$  at the  $j$ -th step and the state vector at the  $(j+1)$ -th step are calculated as

$$\mathbf{x}_c[j+1] = \mathbf{A}_c \mathbf{x}_c[j] + \mathbf{B}_c \mathbf{u}_c[j] \tag{9}$$

$$\mathbf{y}_c[j] = \mathbf{C}_c \mathbf{x}_c[j] + \mathbf{D}_c \mathbf{u}_c[j] \tag{10}$$

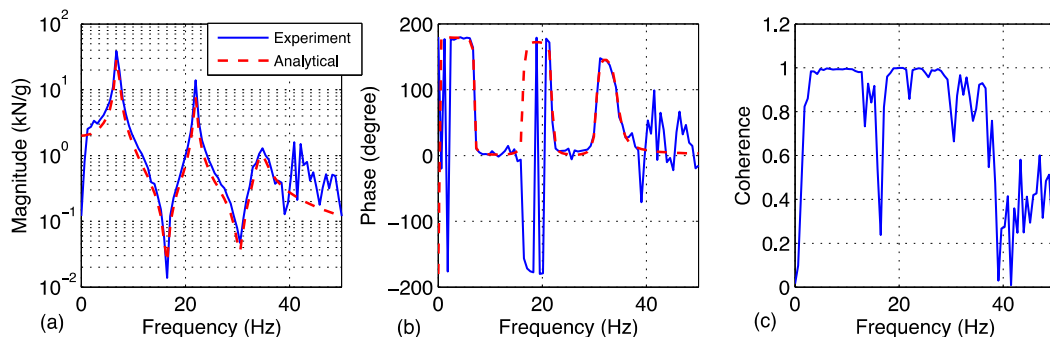


Fig. 6 Frequency response curve and coherence from the table acceleration to measured base shear

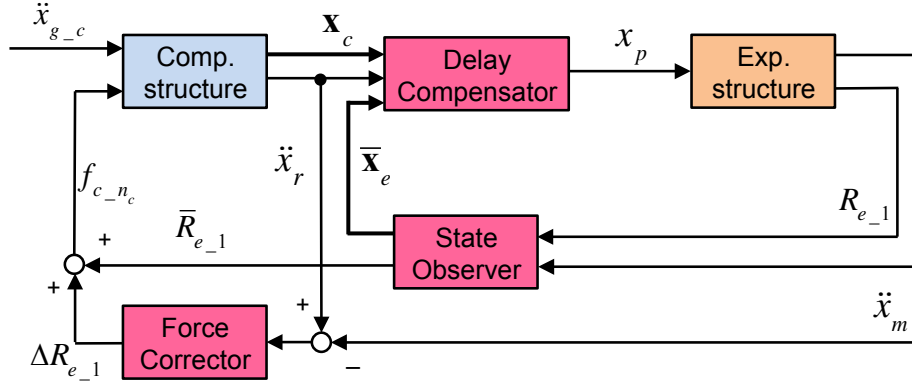


Fig. 7 A block diagram of the substructure shake table test system with compensation techniques for experimental errors

where  $\mathbf{A}_c, \mathbf{B}_c, \mathbf{C}_c$  and  $\mathbf{D}_c$  are the discrete-time system, input, output and feed through matrices of the computational substructure, respectively; The input vector consists of the ground acceleration and the interface force from the experimental substructure, and the output vector consists of the top floor absolute acceleration and displacement of the computational substructure. That is

$$\mathbf{u}_c[j] = \begin{bmatrix} \ddot{x}_g[j] & f_{c-n_c}[j] \end{bmatrix}^T \tag{11}$$

$$\mathbf{y}_c[j] = \begin{bmatrix} \ddot{x}_{c-n_c}[j] + \ddot{x}_{g-c}[j] & x_{c-n_c}[j] + x_{g-c}[j] \end{bmatrix}^T \tag{12}$$

Note that the entries in the output vectors in Eq. (12) are requisite minimums for the proposed procedure in this study. Using the above state space representation, the response of the computational substructure is simulated incorporating the interaction force from the experimental substructure. The output at the  $j$ -th step is used in the following actuator delay compensation technique.

### 5.2 State observer and Kalman filter

If the top floor absolute displacement,  $x_{c-n_c}[j] + x_{g-c}[j]$ , is sent to the shake table controller as the reference at the  $j$ -th step, the measured table acceleration,  $\ddot{x}_m[j]$ , at this step will not match the reference acceleration  $\ddot{x}_r[j]$  that is the top floor absolute acceleration,  $\ddot{x}_{c-n_c}[j] + \ddot{x}_{g-c}[j]$ , due to the inherent actuator delay. To reduce the input acceleration errors caused by the actuator delay, a delay compensation technique needs to be implemented. This study adopts a model-based delay compensation technique that is similar to Carrion and Spencer (2007). The difference is that the

complete state of the experimental substructure that is required for the initial conditions in the delay compensation process is not available in the substructure shake table testing; while all of the nodal displacements and velocities are known at the end of each step in the conventional real-time hybrid simulation, not all of the structural responses are available in the substructure shake table testing because they are neither computed in the computational process nor measured in the experimental process. Therefore, a state observer using Kalman filter is adopted to estimate the state variables for the experimental substructure.

With the measured input  $u_e$  and output  $y_e$  in the experiment and the estimated state vector  $\bar{x}_e$  at the  $j$ -th step, the state vector at the  $(j+1)$ -th step can be estimated as

$$\bar{x}_e[j+1] = (\mathbf{A}_e - \mathbf{L}\mathbf{C}_e)\bar{x}_e[j] + (\mathbf{B}_e - \mathbf{L}\mathbf{D}_e)u_e[j] + \mathbf{L}y_e[j] \quad (13)$$

where  $\mathbf{A}_e$ ,  $\mathbf{B}_e$ ,  $\mathbf{C}_e$  and  $\mathbf{D}_e$  are the discrete-time system, input, output and feed through matrices of the analytical experimental substructure, respectively; and  $\mathbf{L}$  is the Kalman gain. The Kalman gain is determined based on estimates for the covariance of the experimental measurement and process noises along with the accuracy of the model for experimental substructure. The measured input and output in the experiment are the shake table acceleration and the base shear, respectively.

$$u_e[j] = \ddot{x}_{g\_e}[j] \quad (14)$$

$$y_e[j] = R_{e\_1}[j] \quad (15)$$

Furthermore, the measured output in the experiment can be filtered to reduce the influence of the process and measurement noises as

$$\bar{R}_{e\_1}[j] = \bar{y}_e[j] = \mathbf{C}_e\bar{x}_e[j] + \mathbf{D}_e u_e[j] \quad (16)$$

Where  $\bar{R}_{e\_1}$  is the filtered base shear in the experiment that is used in the force correction technique.

### 5.3 Model-based actuator delay compensation

The idea of the model-based delay compensation technique is to predict the future response of the entire structure and send the reference displacement to the shake table ahead of time. If the actuator delay constant is  $\delta t$  and the sampling in the iteration process is  $dt$ , the number of required iterations is  $h = \delta t / dt$ . The iteration sampling,  $dt$ , has to be selected such that the number of iterations,  $h$ , can be completed within the simulation sampling, (i.e. a single time step in the RTHS). The model-based delay compensation begins with initialization of the input and state vectors

$$\hat{u}_e[0, j] = \mathbf{P}_1 y_c[j] = \ddot{x}_{c\_n_c}[j] + \ddot{x}_{g\_c}[j] \text{ where } \mathbf{P}_1 = \begin{bmatrix} 1 & 0 \end{bmatrix} \quad (17)$$

$$\hat{\mathbf{x}}_e[0, j] = \bar{\mathbf{x}}_e[j] \quad (18)$$

$$\hat{\mathbf{x}}_c[0, j] = \mathbf{x}_c[j] \quad (19)$$

Then, the processes at the  $k$ -th iteration ( $k=0, \dots, h$ ) in the delay compensation technique for the  $j$ -th step reference displacement to the shake table are expressed as

$$\hat{\mathbf{x}}_e[k+1, j] = \mathbf{A}_e \hat{\mathbf{x}}_e[k, j] + \mathbf{B}_e \hat{\mathbf{u}}_e[k, j] \quad (20)$$

$$\hat{\mathbf{y}}_e[k, j] = \mathbf{C}_e \hat{\mathbf{x}}_e[k, j] + \mathbf{D}_e \hat{\mathbf{u}}_e[k, j] \quad (21)$$

$$\hat{\mathbf{u}}_c[k, j] = \begin{bmatrix} \ddot{x}_{g\_c}[j+k] & \hat{\mathbf{y}}_e[k, j] \end{bmatrix}^T \quad (22)$$

$$\hat{\mathbf{x}}_c[k+1, j] = \mathbf{A}_c \hat{\mathbf{x}}_c[k, j] + \mathbf{B}_c \hat{\mathbf{u}}_c[k, j] \quad (23)$$

$$\hat{\mathbf{y}}_c[k, j] = \mathbf{C}_c \hat{\mathbf{x}}_c[k, j] + \mathbf{D}_c \hat{\mathbf{u}}_c[k, j] \quad (24)$$

$$\hat{\mathbf{u}}_e[k+1, j] = \mathbf{P}_1 \hat{\mathbf{y}}_c[k, j] \quad (25)$$

The delay compensation technique repeats the above processes (Eqs. (20)-(25))  $h$  times for every simulation time step  $j$ . At the end of the  $h$ -th iteration, the predicted displacement to the shake table at the  $j$ -th step,  $x_p$ , is specified as

$$x_p[j] = \mathbf{P}_2 \hat{\mathbf{y}}_c[h, j] = \hat{x}_{c\_nc}[h, j] + x_{g\_c}[j+h] \text{ where } \mathbf{P}_2 = \begin{bmatrix} 0 & 1 \end{bmatrix} \quad (26)$$

Where  $\hat{x}_{c\_nc}[h, j]$  is the top floor relative displacement of the computational substructure at the  $h$ -th future step predicted from the current  $j$ -th simulation step; and  $x_{g\_c}[j+h]$  is the ground displacement at the computational substructure at the  $(j+h)$ -th step.

#### 5.4 Corrector for errors in base shear induced by input acceleration errors

To reduce the effect of erroneous response in the base shear induced by the propagation of the input acceleration error, the force correction technique is implemented as a part of the substructure shake table testing. Dynamics of the propagation of the input error can be expressed as

$$\tilde{\mathbf{x}}_e[j+1] = \mathbf{A}_e \tilde{\mathbf{x}}_e[j] + \mathbf{B}_e \tilde{\mathbf{u}}_e[j] \tag{27}$$

$$\tilde{\mathbf{y}}_e[j] = \mathbf{C}_e \tilde{\mathbf{x}}_e[j] + \mathbf{D}_e \tilde{\mathbf{u}}_e[j] \tag{28}$$

where  $\tilde{\mathbf{u}}_e$ ,  $\tilde{\mathbf{y}}_e[j]$  and  $\tilde{\mathbf{x}}_e$  are the input, output, and state vector for the error correction process. The input and output in this process can be expressed as

$$\tilde{\mathbf{u}}_e[j] = \ddot{\mathbf{x}}_r[j] - \ddot{\mathbf{x}}_m[j] \tag{29}$$

$$\tilde{\mathbf{y}}_e[j] = \Delta \mathbf{R}_{e\_1}[j] \tag{30}$$

where  $\ddot{\mathbf{x}}_r - \ddot{\mathbf{x}}_m$  is the input acceleration error and  $\Delta \mathbf{R}_{e\_1}$  is the erroneous base shear induced by the input acceleration error. The corrected force is the sum of the filtered and error-induced base shear as

$$\mathbf{f}_{c\_n_c}[j] = \bar{\mathbf{R}}_{e\_1}[j] + \Delta \mathbf{R}_{e\_1}[j] \tag{31}$$

This corrected force is used in the computational process in Eq. (11), and the substructure shake table test system is now completely closed.

## 6. Experimental results

All of the developed techniques for substructure shake table testing are implemented in the control system at the Johns Hopkins University. A series of substructure shake table tests are conducted using the techniques developed in this study. It should be mentioned that the same series of substructure shake table tests were attempted without the developed techniques. However, tests could not be completed because of stability issues, and comparable and representable results were not obtained. Therefore, the test results presented in this section are only those with the developed techniques. Data from the tests can be accessed in Nakata and Stehman (2014). Basic parameters for the simulation are as follows: sampling of the entire simulation,  $0.004s$ ; actuator delay,  $\delta t = 0.068 s$ ; sampling of the iteration process in the delay compensation technique,  $dt = 0.004s$ ; and number of iterations in the delay compensation,  $h = 17$ .

### 6.1 Harmonic ground excitation inputs

The first series of tests presented here are harmonic ground excitation tests. The main objectives of the harmonic excitation tests are to assess stability, propagation of errors, and validity of the substructure shake table testing. Fig. 8 shows the entire and zoomed sections of the acceleration and base shear time histories when the entire structure is subjected to 10 cycles of 2.0 Hz harmonic ground motion with the peak ground acceleration of 0.041 g and the peak ground

displacement of 2.54 mm. For a comparative purpose, results from a pure numerical simulation are also shown in the plots.

Firstly, it can be observed from Fig. 8(a) that the measured acceleration tracks the reference acceleration well in a large simulation time scale. The zoomed section of the acceleration in Fig. 8(b) also reveals that reasonable acceleration tracking at 2.0 Hz is achieved. However, the measured acceleration contains high frequency vibrations that are not present in the reference and numerical accelerations. Note that the reference acceleration is the one that is computed in the substructure shake table test whereas the numerical acceleration is from pure numerical simulation. Because the substructure shake table test incorporates the experimental base shear, the reference acceleration has some discrepancy from the numerical acceleration. It should be pointed out that the peak time of the measured acceleration matches that of the reference, demonstrating effectiveness of the model-based delay compensation technique. The difference between the reference and measured accelerations is the input acceleration error of which effect on the base shear is for accounted in this substructure shake table test.

Figs. 8(c) and 8(d) show that the measured base shear is mostly 2.0 Hz harmonic. However, as can be seen in Fig. 8(d), the measured base shear also contains vibration at approximately 20 Hz. The measured base shear is filtered and then corrected based on the input acceleration error during the substructure shake table testing. The corrected base shear shows very good agreement with the numerical base shear. Although the numerical base shear is not a reference that has to be followed, this agreement and smoothness in the corrected base shear indicates that the errors due to process and measured noises as well as those that are induced by the input acceleration errors are effectively reduced by the error compensation techniques in the substructure shake table testing.

A comparison between the substructure shake table test (labeled as 'Hybrid') and the numerical simulation in terms of structural responses under the 2.0 Hz harmonic excitation is shown in Fig. 9. Relative displacement, absolute displacement, and absolute acceleration at the 2<sup>nd</sup>, 6<sup>th</sup>, and 10<sup>th</sup> floors are shown in the plots. Note that the displacement responses at the 10<sup>th</sup> floor (the top floor of the experimental substructure) are recovered from the acceleration response. These plots illustrate several important features of the substructure shake table test that can be summarized as follows: while some discrepancies between the substructure shake table test and the numerical simulation are seen at floors in the experimental substructure, almost all of the structural responses in the substructure shake table test show very good agreement with those in the numerical simulation. Furthermore, it can be seen that all types of responses show gradual increase with the increase of the floor number. Because the input frequency of 2.0 Hz is relatively close to the first natural frequency of the entire structure, overall structural responses in the substructure shake table test seem reasonable, meaning that the structural responses at the first vibration mode or equivalent can be accurately simulated. Thus, the substructure shake table test here provides promising results as a potential means to simulate the structural responses.

Next, simulation results under a harmonic ground excitation at 6.0 Hz that is close to the second natural frequency of the entire structure is presented. Fig. 10 shows the entire and zoomed sections of the acceleration and base shear time histories when the entire structure is subjected to 10 cycles of 6.0 Hz harmonic ground motion with the peak ground acceleration of 0.11 g and the peak ground displacement of 0.76 mm. Unlike in the previous simulation, the acceleration time histories in Figs. 10(a) and 10(b) show large discrepancy with the reference acceleration, containing high frequency vibration of approximately 30 Hz. Because of the poor acceleration tracking, the input acceleration errors are present at this frequency as expected from the observation in the previous section.

The measured base shear shown in Figs. 10(c) and 10(d) has large discrepancy with the numerical base shear. However, despite the large differences, the corrected base shear shows good agreement with the numerical base shear. This agreement is because the erroneous responses in the measured base shear are mostly induced by the input acceleration errors, and the propagation of the input acceleration errors is accurately traced by the techniques developed in this study. Thus, the proposed compensation techniques are shown to be effective even with a significant level of input acceleration errors.

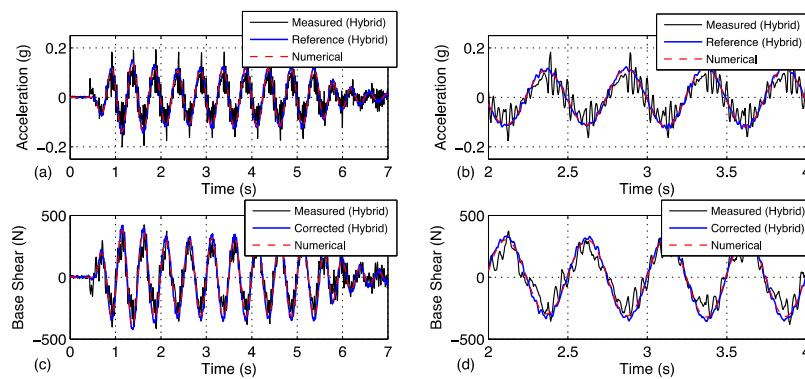


Fig. 8 Acceleration and base shear time histories under 2.0 Hz harmonic ground excitation: (a) the entire acceleration time histories; (b) a zoomed section of the acceleration time histories; (c) the entire base shear time histories; and (d) a zoomed section of the base shear time histories

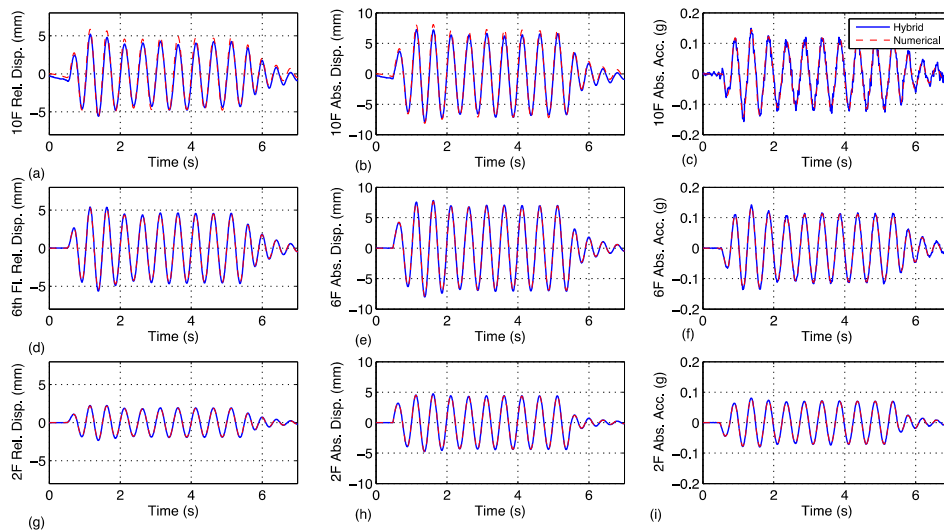


Fig. 9 Structural responses under 2.0 Hz harmonic ground excitation: (a), (d), and (g), relative floor displacement at the 10<sup>th</sup>, 6<sup>th</sup> and 2<sup>nd</sup> floor, respectively; (b), (e), and (h), absolute floor displacement at the 10<sup>th</sup>, 6<sup>th</sup> and 2<sup>nd</sup> floor, respectively; and (c), (f), and (i), absolute floor acceleration at the 10<sup>th</sup>, 6<sup>th</sup> and 2<sup>nd</sup> floor, respectively

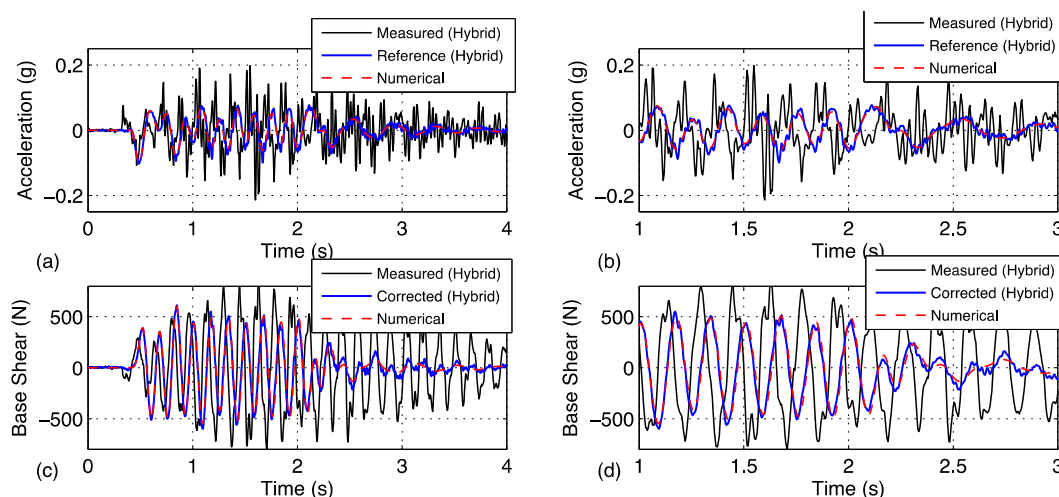


Fig. 10 Acceleration and base shear time histories under 6.0 Hz harmonic ground excitation: (a) the entire acceleration time histories; (b) a zoomed section of the acceleration time histories; (c) the entire base shear time histories; and (d) a zoomed section of the base shear time histories

Structural responses under the 6.0 Hz harmonic excitation are shown in Fig. 11. As is the case with the previous simulation with the 2.0 Hz excitation, discrepancies between the substructure shake table test and the numerical simulation are seen at floors in the experimental substructure. But, good agreement between the substructure shake table test and the numerical simulation in terms structural responses is also obtained in this simulation with the 6.0 Hz excitation. It is interesting to see that the 6<sup>th</sup> floor accelerations are smaller than those at the 2<sup>nd</sup> floor and do not contain much of the 6.0 Hz vibration despite of the 6.0 Hz excitation frequency. This observation seems to make sense because the input frequency of 6.0 Hz is close to the second natural frequency of the entire structure; the 6<sup>th</sup> floor is close to a node in the second vibration mode. Thus, the test results here demonstrate that the overall responses of the entire structure under a relative high frequency around the second natural frequency are also simulated reasonably well using the substructure shake table test.

The experimental simulations using harmonic excitations in this section proved that though experimental errors including input acceleration errors are present, the substructure shake table tests are successfully completed using the developed compensation techniques. The substructure shake table tests are stable and valid, indicating that experimental errors are not propagated through the real-time hybrid simulation processes.

## 6.2 Earthquake ground excitation input

Substructure shake table tests are performed using earthquake ground excitations. In this paper, results from the 1995 Kobe earthquake are presented and discussed.

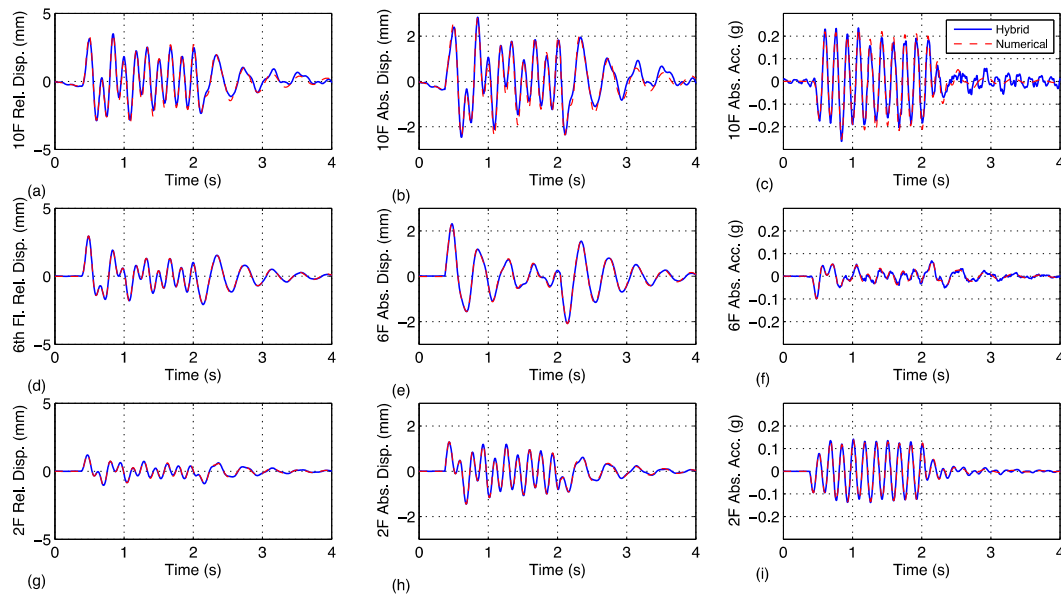


Fig. 11 Structural responses under 6.0 Hz harmonic ground excitation: (a), (d), and (g), relative floor displacement at the 10th, 6th and 2nd floor, respectively; (b), (e), and (h), absolute floor displacement at the 10th, 6th and 2nd floor, respectively; and (c), (f), and (i), absolute floor acceleration at the 10th, 6th and 2nd floor, respectively

Fig. 12 shows the entire and zoomed sections of the acceleration and base shear time histories when the entire structure is subjected to the 1995 Kobe earthquake with the peak ground acceleration of 0.23 g and the peak ground displacement of 17.8 mm. The measured acceleration shows good tracking to the primary low frequency vibrations in the reference acceleration including the phase characteristics. However, notable high frequency vibrations due to the imperfect acceleration tracking can also be observed. It should be mentioned that while tracking performance is improved with the increase of the excitation level, input acceleration errors are still unavoidable due to the imperfection of the acceleration tracking. As in the case with the previous harmonic excitation simulations, the measured base shear shows discrepancy with the numerical base shear. However, once the influence of the input acceleration errors is addressed, the corrected base shear agrees well with the numerical base shear. This good agreement demonstrates that the developed compensation techniques effectively reduce the influence of the experimental errors during the earthquake excitation simulation.

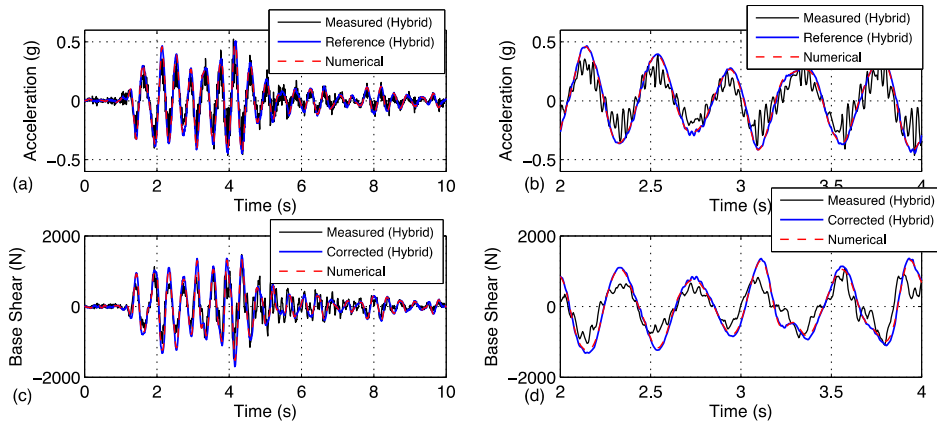


Fig. 12 Acceleration and base shear time histories under the 1995 Kobe earthquake excitation: (a) the entire acceleration time histories; (b) a zoomed section of the acceleration time histories; (c) the entire base shear time histories; and (d) a zoomed section of the base shear time histories

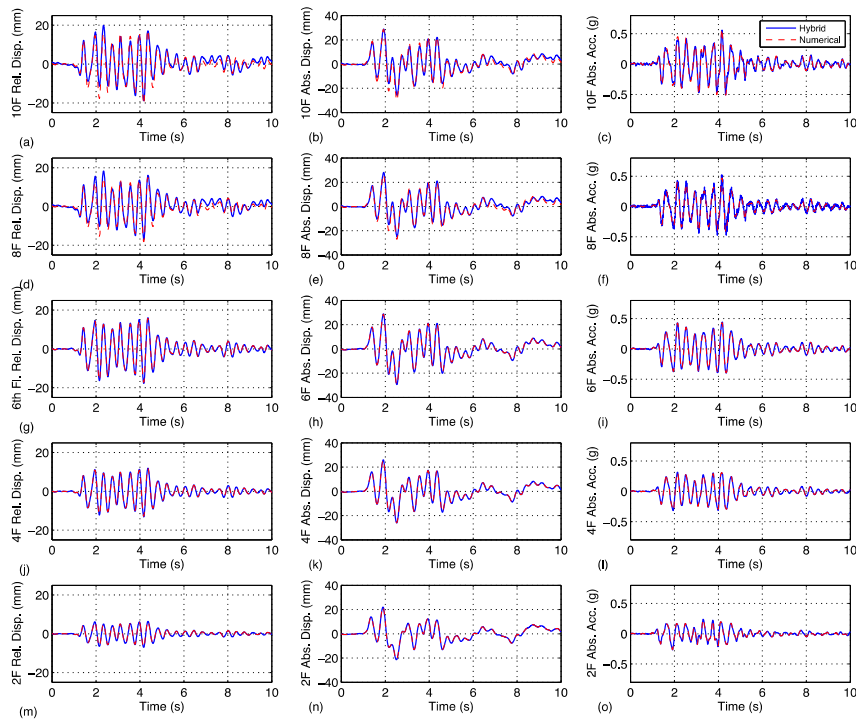


Fig. 13 Structural responses under the 1995 Kobe earthquake excitation: (a), (d), (g), (j), and (m), relative displacement at the even floors from top to bottom (10th to 2nd); (b), (e), (h), (k), and (n), absolute displacement at the even floors from top to bottom (10th to 2nd); and (c), (f), (i), (l), and (o), absolute displacement at the evenfloors from top to bottom (10th to 2nd)

Fig. 13 shows the structural responses under the Kobe earthquake during the substructure shake table test. Relative displacement, absolute displacement and absolute acceleration at the even floors are shown in the plots. It can be seen that while some discrepancies between the substructure shake table testing and the numerical simulation are seen at the upper floor responses, the overall structural responses in the substructure shake table test show good agreement with the numerical simulation. The responses of each type are approximately proportional with the increase of floor number, indicating that the entire structural responses are mostly the first vibration mode. This observation seems reasonable because the primary frequency of this earthquake is close to the first natural frequency. Thus, the simulation results here demonstrate that the substructure shake table testing with the developed compensation techniques for experimental errors successfully simulate the response of the 10<sup>th</sup>-story structure under the earthquake ground excitation input. It should be mentioned that although results are not presented in the paper, more substructure shake table tests were conducted using different earthquakes and the same level of agreement with numerical simulation are obtained.

## 7. Conclusions

This study presented a real-time hybrid simulation technique using shake tables including compensation techniques for experimental errors. The developed techniques included compensation techniques for response errors induced by erroneous input acceleration, model-based actuator delay compensation with state observer, and force correction using Kalman filter. The effectiveness of those techniques was experimentally verified through a series of RTHS using a uni-axial shake table and three-story steel frame structure at the Johns Hopkins University.

While the paper presented mostly successful parts of the study, unbiased fair discussions need to be provided. To pursue further research along this direction, remaining challenges that have to be addressed in the future study are listed below.

- As demonstrated, the substructure shake table testing with the developed techniques made it possible to perform reliable simulations that were not possible without them. However, it is owing to a relatively large damping of the computational structure to some extent. When the RTHS using shake table were performed using computational structures with smaller damping, simulations were unstable with and without the compensation techniques. In the future, the compensation techniques have to be further refined to take effects under more strict conditions.
- The compensation techniques for response errors induced by the input acceleration errors were effective even if the input errors were significant. This is because the test structure had high correlation between the ground acceleration and the base shear. If test structures are nonlinear or have less correlation between the ground shaking and the response, the same level of improvement cannot be expected. Future research needs to address such limitations in the current approach. A possible approach is the model updating technique that can capture nonlinearities of the experimental model.
- In this study, efforts to improve acceleration tracking have not been thoroughly addressed. Future studies have to address the improvement of the acceleration tracking errors.

While challenges are still remaining, this study addressed the issues of the response errors induced by erroneous and inevitable input acceleration errors in RTHS using shake tables and developed compensation techniques for such experimental errors. The authors believe that the

developed compensation techniques can serve as the initial effort to address such inevitable experimental errors.

## Acknowledgements

This research is supported by the National Science Foundation under an award entitled “CAREER: Advanced Acceleration Control Methods and Substructure Techniques for Shaking Table Tests (grand number CMMI- 0954958)”.

## References

- Carrion, J. and Spencer, B.F. (2007), *Model-based strategies for real-time hybrid testing*, NSEL report, University of Illinois at Urbana-Champaign, NSEL-006.
- Carrion, J.E., Spencer, B.F. and Phillips, B.M. (2009), “Real-time hybrid simulation for structural control performance assessment”, *Earthq. Eng. Eng. Vib.*, **29**(8), 481-492.
- Christenson, R., Lin, Y., Emmons, A. and Bass, B. (2008), “Large-scale experimental verification of semiactive control through real-time hybrid simulation1”, *J. Struct. Eng. - ASCE*, **134**(4), 522-534.
- Dyke, S., Spencer, B., Quast, P. and Sain, M. (1995), “Role of control-structure interaction in protective system design”, *J. Eng. Mech. - ASCE*, **121**(2), 322-338.
- Günay, M.S. and Mosalam, K.M. (2012), “Investigation of the response of electrical insulator posts using real-time hybrid simulation on a smart shaking table”, *Proceedings of the 15<sup>th</sup> World Conference on Earthquake Engineering*, Lisbon, Portugal.
- Igarashi, A., Iemura, H. and Suwa, T. (2000), “Development of substructured shaking table test method”, *Proceedings of the 12th World Conference on Earthquake Engineering*, Auckland, New Zealand.
- Igarashi, A., Sanchez-Flores, F., Iemura, H., Fujii, K. and Toyooka, A. (2009). “Real-time hybrid testing of laminated rubber dampers for seismic retrofit of bridges”, *Proceedings of the 3rd International Conference on Advances in Experimental Structural Engineering*, San Francisco, USA.
- Ji, X., Kajiwara, K., Nagae, T., Enokida, R. and Nakashima, M. (2009), “A substructure shaking table test for reproduction of earthquake responses of high-rise buildings”, *Earthq. Eng. Struct. D.*, **38**(12), 1381-1399.
- Lee, S., Parka, E., Mina, K. and Park, J. (2007), “Real-time substructuring technique for the shaking table test of upper substructures”, *Eng. Struct.*, **29**(9), 2219-2232.
- Nakashima, M., Kato, H. and Takaoka, E. (1992), “Development of real-time pseudo dynamic testing”, *Earthq. Eng. Struct. D.*, **21**(1), 79-92.
- Nakata, N. (2010), “Acceleration tracking control for earthquake simulators”, *Eng. Struct.*, **32**(8), 2229-2236.
- Nakata, N. (2012), “A multi-purpose earthquake simulator and a flexible development platform for actuator controller design”, *J. Vib. Control*, **18**(10), 1552-1560.
- Nakata, N. and Stehman, M. (2012), “Substructure shake table test method using a controlled mass:formulation and numerical simulation”, *Earthq. Eng. Struct. D.*, **41**(14), 1977-1988.
- Nakata, N. and Stehman, M. (2014), “Substructure shake table testing of 10-story RTHS structure”, *Network for Earthquake Engineering Simulation (NEES)*(distributor). Dataset. DOI: 10.4231/D3ST7DX1R.
- Neild, S.A., Stoten, D.P., Drury, D. and Wagg, D.J. (2005), “Control issues relating to real-time substructuring experiments using a shaking table”, *Earthq. Eng. Struct. D.*, **34**(9), 1171-1192.
- Pan, P., Nakashima, M. and Tomofuji, H. (2005), “Online test using displacement-force mixed control”, *Earthq. Eng. Struct. D.*, **34**(8), 869-888.
- Phillips, B.M. and Spencer, B.F. (2011), “Model-based feedforward-feedback actuator control for real-time hybrid simulation”, *J. Struct. Eng. - ASCE*, **139**, 1205-1214.
- Shao, X., Reinhorn, A.M. and Sivaselvan, M.V. (2011), “Real-time hybrid simulation using shake tables and

- dynamic actuators”, *J. Struct. Eng. -ASCE*, **137**(7), 748-760.
- Spencer, B. and Yang, G. (1998), “Earthquake simulator control by transfer function iteration”, *Proceedings of the 12<sup>th</sup> ASCE Engineering Mechanics Conference*, San Diego, USA.
- Stehman, M. and Nakata, N. (2012), “Direct acceleration feedback control of shake tables with force stabilization”, *J. Earthq. Eng.*, **17**(5), 736-749.
- Stoten, D. P. and Gómez, E. (2001), “Adaptive control of shaking tables using the minimal control synthesis algorithm”, *Philos. T. R. Soc. A*, **359**(1786), 1697-1723.
- Twitchell, B. and Symans, M. (2003), “Analytical modeling, system identification, and tracking performance of uniaxial seismic simulators”, *J. Eng. Mech. - ASCE*, **129**(12), 1485-1488.
- Zapateiro, M., Karimi, H.R., Luo, N. and Spencer, B.F. (2010), “Real-time hybrid testing of semi active control strategies for vibration reduction in a structure with MR damper”, *Struct. Control Health Monit.*, **17**(4), 427-451.

**Notation**

Variable	Description (in order of appearance)
$n$	Number of stories in the entire structure
$i$	Floor number, $i = c\_i$ for the $i$ -th floor of the computational substructures and $i = e\_i$ for the $i$ -th floor of the experimental substructure
$m_i$	$i$ -th floor mass
$x_i, \dot{x}_i, \ddot{x}_i$	$i$ -th floor structural displacement, velocity and acceleration relative to the base
$R_i$	$i$ -th floor restoring force including stiffness and damping
$d_i, \dot{d}_i$	$i$ -th floor story drift and relative velocity
$\ddot{x}_g$	Ground acceleration input for the entire structure
$n_c$	Number of stories in the computational substructure
$n_e$	Number of stories in the experimental substructure
$f_{c\_n_c}$	Interaction force applied at the top floor of the computational substructure
$\ddot{x}_{g\_c}, x_{g\_c}$	Ground acceleration and displacement for the computational substructure
$\ddot{x}_{g\_e}$	Ground acceleration input for the experimental substructure
$j$	Iteration number during the substructure shake table test
$(\mathbf{A}_c, \mathbf{B}_c, \mathbf{C}_c, \mathbf{D}_c)$	State space matrices for the computational substructure
$\mathbf{u}_c, \mathbf{x}_c, \mathbf{y}_c$	Input, state and output vectors for the computational substructure during RTHS
$\ddot{x}_r$	Reference acceleration for shake table
$\ddot{x}_m$	Measured shake table acceleration
$(\mathbf{A}_e, \mathbf{B}_e, \mathbf{C}_e, \mathbf{D}_e)$	State space matrices for the experimental substructure model
$\mathbf{L}$	Kalman gain for experimental state estimator
$\mathbf{u}_e$	Input to experimental state estimator
$y_e$	Measured output from physical experimental substructure
$\bar{\mathbf{x}}_e, \bar{y}_e$	Estimated state and output from experimental state estimator
$\bar{R}_{e\_1}$	Kalman filtered base shear from experimental substructure
$\delta t$	Linearized actuator delay constant
$dt$	Sampling time for iterative delay compensation
$h$	Required number of iterations for actuator delay compensator
$k$	Iteration number of delay compensator
$\hat{\mathbf{u}}_e$	Input to experimental substructure model in delay compensator
$\hat{\mathbf{x}}_e, \hat{y}_e$	Experimental state vector and output in delay compensator

---

$\hat{\mathbf{x}}_c, \hat{\mathbf{y}}_c$	Computational state and output vectors in delay compensator
$x_p$	Predicted top floor displacement of computational substructure
$\hat{x}_{c_{-}n_c}$	Future top floor displacement of computational structure used in delay compensator
$\tilde{u}_e, \tilde{\mathbf{x}}_e, \tilde{y}_e$	Input, state and output from experimental force corrector
$\Delta R_{e\_1}$	Error in measured experimental base shear

---